Journal of Cleaner Production 418 (2023) 138042

Contents lists available at ScienceDirect

Journal of Cleaner Production

journal homepage: www.elsevier.com/locate/jclepro

Rapid and accurate quality assessment method of recycled food plastics VOCs by electronic nose based on Al-doped zinc oxide

Valeriy Zaytsev [a,1], Fedor S. Fedorov [a,*,1], Boris Goikhman [a,2], Alexander Maslennikov [b], Vasilii Mashukov [c], Nikolay P. Simonenko [d], Tatiana L. Simonenko [d], Dinara Gabdullina [c], Olga Kovalenko [c], Elizaveta P. Simonenko [d], Polina Kvitko [c], Olga Penkova [e], Dina Satybaldina [f], Shakhmaran Seilov [f], Tatiana S. Dubinina [a], Dmitry A. Gorin [a], Albert G. Nasibulin [a,**]

[a] Skolkovo Institute of Science and Technology, 3 Nobel str., 121205, Moscow, Russia
[b] SIBUR LLC, 16/1 Krzhizhanovskiy str., 117218, Moscow, Russia
[c] SIBUR PolyLab LLC, Skolkovo Innovation Center 2 Bolshoy Boulevard, 121205, Moscow, Russia
[d] Kurnakov Institute of General and Inorganic Chemistry of the Russian Academy of Sciences, 31 Leninsky pr., 119991, Moscow, Russia
[e] NIOST LLC, 2 bld. 270 Kuzovlevsky Tract, 634022, Tomsk, Russia
[f] L.N. Gumilyov Eurasian National University, 2 Satpayev str., 010008, Astana, Kazakhstan

ARTICLE INFO

Handling Editor: Zhen Leng

Keywords:
Plastics
Polymer odors assessment
Al-doped zinc oxide
Electronic nose
Machine learning protocols.

ABSTRACT

Plastic recycling technologies are being actively developed and implemented to cope with increasing volume of plastic. Such technologies require new analytical tools able to control the quality of the recycled polymers to be further integrated in production processes. Here, we propose a rapid and selective quality assessment method for polymer materials made of high-density polyethylene using electronic nose with aluminum doped zinc oxide sensing material in combination with the *RandomForestClassifier* machine learning tool. We test total content of volatile organic compounds both odor-active responsible for the smell and odorless of primary and secondary plastics, and evaluate corresponding organic vapors emitted by the plastics by headspace gas chromatography and mass-spectrometry at optimized conditions like sample temperature, sensor signal recovery time. The electronic nose demonstrated the good correlation of vector signal with the emitted volatile compounds with an accuracy more than 98.5% when discriminating between primary and secondary plastics. Addition of zeolites to the recycled plastic is shown to decrease the appearance of off-odors.

1. Introduction

Severe use of plastic (Khanam and AlMaadeed, 2015; Mark, 2007; Sangroniz et al., 2019; Seitz, 1993; World et al., 2018), even though it is deeply incorporated in daily life, leaves a huge mark on the landscape of the Earth. The annual consumption of polymer composites reaches about 260 megatons according to a 2020's report ('Polymer Market Analysis: Plant Capacity, Production, Operating Efficiency, Demand & Supply, Product Type, Application, Distribution Channel, Region, Competition, Trade, Market Analysis, 2015–2030', 2021), with a projected increase to 430 megatons by 2030. Such a massive increase in polymer production to meet the growing demand of the Earth's population makes a major impact on soils (Chae and An, 2018; Nel and Froneman, 2015), marine waters (Pabortsava and Lampitt, 2020), and mammals (Yates et al., 2021) with plastic residuals found even in human blood (Leslie et al., 2022). At the same time, the share of recycled plastics (Häußler et al., 2021; Rahimi and Garciá, 2017; Rajendran et al., 2012) is only 14% of the total consumption, while the rest goes to the polymer waste (Zheng and Suh, 2019), although the part of potentially recyclable plastics is higher than 80% of the total amount of produced plastics (Patoski, 2019). The insufficient recycling of plastics is on top of this problem affecting the quality of the sanitary and epidemiological state of the final product (Hahladakis et al., 2018; Nerín et al., 2016). A great amount of unrecycled plastics envelops a "Plastic waste Era" (Ball,

* Corresponding author.
** Corresponding author.
E-mail addresses: f.fedorov@skol.tech (F.S. Fedorov), a.nasibulin@skol.tech (A.G. Nasibulin).
[1] These authors contributed equally to this work.
[2] current affiliation: Electrical and Computer Engineering Department, Technion—Israel Institute of Technology, Haifa 32000, Israel.

https://doi.org/10.1016/j.jclepro.2023.138042
Received 19 December 2022; Received in revised form 6 June 2023; Accepted 8 July 2023
Available online 10 July 2023

2020; Van Rensburg et al., 2020) of our civilization. To be harmonized by recycling protocols, we should develop methods of rapid and precise analysis of the quality of polymeric materials (Lok et al., 2020; Schwartz-Narbonne et al., 2023), especially when they are utilized in the food and pharmaceutical industries (Garcia and Robertson, 2017; Vollmer et al., 2020).

Quality control methods of polymers are prescribed by regulations and acts of food and drug administration agencies, in particular by US FDA ('Recycled Plastics in Food Packaging', 2020), and based on internationally certified standards like ISO (*ISO/DIS 5677 Testing and characterization of mechanically recycled Polypropylene (PP) and Polyethylene (PE) for intended use in different plastics processing techniques*, 2022, *ISO 13741-1:1998 Plastics/rubber — Polymer dispersions and rubber latices (natural and synthetic) — Determination of residual monomers and other organic components by capillary-column gas chromatography*, 1998, *ISO 3251:2019 Paints, varnishes and plastics — Determination of non-volatile-matter content*, 2019). Gas chromatography (Demets et al., 2020; Vera et al., 2020) with various detection options as well as IR spectroscopy (Giron and Celina, 2017) are often employed for the assessment of the plastic quality. These methods enable the evaluation of vapors that constitute a smell of plastics, an important quality characteristic, especially in the case of secondary plastics. For example, the smell of waste plastics was tested by using three sampling methods such as solid–phase microextraction and two different purge and trap methods, based on sampling on the activated charcoal followed the carbon disulfide desorption or on the Tenax-TA followed the thermal desorption technique, to be further analyzed by gas chromatography on pair with mass spectrometry (Demets et al., 2020). The appearance of off-odors related to primary and secondary plastics, both as-recycled or in a compound, can be also evaluated by trained personnel, i.e. a panel of experts.

An objective analysis of plastic smell might be conducted using gas analytical units like "electronic noses", or e-noses (Cabanes et al., 2020; Wiedmer et al., 2017), as it is often applied for food quality control (Fedorov et al., 2021; Tan and Xu, 2020), electronic sommelier (Vera et al., 2010; Yu et al., 2014), classification of close homologs and isomers (Goikhman et al., 2022), etc. The electronic nose usually represents an array of sensors with good cross-sensitivity those vector signal, when processed by pattern recognition algorithms, e.g., using machine learning, is specific to an analyte or mixture. Accordingly, the operation of the e-nose is designed to be similar to the mammalian olfactory system (Gardner and Bartlett, 1994; Han et al., 2022; Persaud and Dodd, 1982; Potyrailo, 2016) with the difference that the e-nose sensors give a response to the total content of volatile substances they are sensitive to when compared to the mammalian nose, which is able to recognize only odor-active volatiles that specifically bind to proteins in the nasal mucosa (Buck and Axel, 1991; Pelosi, 1996). E-nose offers primarily good selectivity, low power consumption, especially for on-chip-made sensor arrays, and rather good rapidness of control.

The VOCs analysis of PET-based primary plastic was first conducted by Torri et al., who studied 25 homo- and copolymers of ethylene and five homo- and copolymers of polypropylene with a commercial e-nose based on 10 metal oxide sensors (Torri et al., 2008). The authors demonstrated confident discrimination between polymer samples based on different amounts of emitted volatile compounds using principal component analysis (PCA). Semiconductor mono- (Bigger et al., 1996) and multisensor systems (Van Deventer and Mallikarjunan, 2002; Yüzay and Selke, 2007) were implemented also for the smell analysis of low-density polyethylene films in conjunction with an alternative assessment by the sensory expertise. An E-nose system based on 8 piezoelectric quartz resonators was also applied to monitor the degradation of primary OXO-biodegradable polyethylene films when exposed to UV and temperature (Kuchmenko et al., 2020). The authors were able to selectively discriminate the OXO-polyethylene film degradation degree by using PCA, which is related to the appearance of volatile organic compounds (VOCs) due to the employed prooxidant additives. Recently, Oleneva et al. described an application of e-nose to check the toxicity of plastic toys, showing an accuracy of around 96% (Oleneva et al., 2020).

However, an analysis of components of the plastic smell and its emission *versus* e-nose selective assessment has not been yet properly performed. Moreover, the smell of secondary plastics, including the plastic compounds with added odor adsorbers, has not yet been examined by this technique.

Thus, in our study, we propose an approach for assessment of the quality of recycled plastics using e-nose followed by smell classification on the basis of machine learning protocols. We demonstrated the high sensitivity of sensors and selective discrimination of smells of polymer samples relative to synthetic air at different temperatures. The accuracy of the classification results for the *Random Forest* algorithm (Xu et al., 2019) was above 98.5%. We also presented that the maximum recognition coefficient (1.0 for pairwise recognition between 3 polymers and synthetic air) between polymer classes is typical for the room temperature analysis, which enhances the advantages regarding the simplicity and rapidness of this approach in comparison with ISO standards. Therefore, our approach opens a new avenue for simple and rapid control of the primary and secondary plastics for the food and pharmaceutical industries.

2. Materials and methods

2.1. Synthesis of functional material

We chose an aluminum-doped zinc oxide (*Al-doped ZnO*), a transparent and conductive material (Bo et al., 2020), due to its proven good sensing properties (Sanger et al., 2019; Van Toan et al., 2021). The synthesis of *Al-doped ZnO* is described elsewhere (Fedorov et al., 2022; Goikhman et al., 2022). Briefly, to synthesize *Al-doped ZnO*, we utilized aqueous $Zn(NO_3)_2{\cdot}6H_2O$ (98%, *Khimmed*, Russia) and $Al(NO_3)_3{\cdot}9H_2O$ (98%, *Khimmed*, Russia) maintaining a total concentration of Zn^{2+} and Al^{3+} ions to be 0.3 M in a ratio to get ZnO - 1.5% Al_2O_3 composition. An aqueous 5 wt% solution of $NH_3{\cdot}H_2O$ (28–30 wt%, *Sigma-Aldrich*) was added at a temperature of 25 °C at a constant rate of 50 μL/s using automatic high precision potentiometric titrator *ATP-02* (*Aquilon JSC*, Russia) to ensure a reproducible precipitation process (until reaching pH = 8, which ensures complete conversion of the used salts with the formation of corresponding hydroxides). The sediment was centrifuged at 15000 rpm for 10 min (*Elmi CM-50* centrifuge, *ELMI laboratory technology*, Latvia), washed with deionized water (after supernatant removal, the sediment was washed three times with the volume of deionized water similar to the volume of supernatant) and dried at 100°C for 3 h following the annealing at 350 °C for 1 h in air. 7 μL of 5% dispersion of the obtained *Al-doped ZnO* particles in a mixture of ethanol C_2H_5OH (95%, *Sigma-Aldrich*) with deionized water H_2O (ν_{C2H5OH}/ν_{H2O} = 1) was drop-cast on multisensor chip and then dried at ca. 80 °C. Scanning electron microscopy images of the deposited *Al-doped ZnO* sensing layer at the chip were acquired using *FEI Teneo VolumeScope* (*FEI Comp.,* the USA) at 20 kV. The images are presented in Fig. S1 in the Supplementary Materials.

2.2. Polymer characterization

In this study, we evaluated the smell of polymer samples based on high-density polyethylene: *Sample #1* is a copolymer of ethylene with hexene-1; *Sample #2* is a recycled polymer with an adsorbent additive to eliminate the influence of VOCs, i.e., off-odors; *Sample #3* is a recycled polyethylene sample. As an adsorbent additive, we applied zeolites (K. P. Veerapandian et al., 2019; Keshavarzi et al., 2015; Li et al., 2021) with a concentration in the range from 0.1 to 2.0 wt %. The plastic samples are represented by cylindrical granules with a length of ~5 mm and a diameter of ~1 mm.

The appearance of emitted compounds was tested using simultaneous thermal analysis, i.e., by differential scanning calorimetry (DSC)

and thermogravimetric analysis (TGA) coupled with mass spectrometry (STA-MS). The tests included gradual heating from 30 °C to 500 °C at a rate of 5 °C per minute in synthetic air. The measurements were carried out using an *STA 449 F3 Jupiter*® simultaneous thermal analysis device combined with a *QMS 403 Aëolos Quadro* quadrupole mass spectrometer (*NETZSCH Gerätebau GmbH*, Germany). For the measurements, the material was encapsulated in an aluminum crucible. A silicon carbide furnace was chosen for the experiments. We evacuated the device prior to each experiment.

We further performed gravimetric tests for these polymers after keeping them under isothermal conditions at temperatures of 50 °C, 75 °C, and 105 °C for 24 h, respectively. The experiment was carried out using the *UT-4630V* installation (*ULAB*, China) at ambient pressure. The polymer samples in granules ($m \approx 15\ g$) were placed in aluminum boats and then exposed to elevated temperatures.

Also, we applied a gas chromatograph *Agilent 7890A* (*Agilent Technologies*, USA) with a mass spectrometric detector *5975C* and a headspace sampler *Agilent HS 7697A* for the qualitative assessment of the content of VOCs in the plastic samples. The polymer granules ($m = 10.0\ g$) were loaded into a vial (the volume is 20 ml), and the sample was thermally equilibrated for 20 min at 70 °C. Then the vapor phase was analyzed once. Each chromatographic peak was indexed using NIST17 mass spectra database to get the qualitative mixture composition. The relative content of each component in the gas mixture is estimated by the normalization of the chromatographic peak area. An unidentified component was a compound whose mass spectrum match was not found in the NIST17 database and/or the probability of its match with the NIST17 library was less than 80%.

The qualitative analysis of the polymer samples was made by Raman spectroscopy at $\lambda = 532$ nm excitation wavelength and the power of 1 mW with x50 objective using *DXR™ xi Raman Imaging Microscope* (*ThermoFisher Scientific*, Waltham, MA, USA). Also, the semi-quantitative analysis was performed by FT-IR spectroscopy using *VERTEX 70v FT-IR Spectrometer* (*Bruker*, USA). For each polymer sample, we obtained the attenuated total reflection spectrum (64 scans) in the wavenumber range of 3500–600 cm^{-1} with a resolution of 2 cm^{-1}.

We used a sensory evaluation method, based on two consecutive tests of polymer vapor inhalation by an expert panel of 6 people, as a comparative method for analyzing the plastic odors of the studied samples. The panel experts are chosen among the people without bad habits and respiratory diseases.

The samples with a mass of ~100 g were preliminarily kept in glass flasks with a volume of 500 ml at (23 ± 2)°C for 24 h. Each polymer sample is estimated by the expert panel against the empty glass flask. The first assessment is given immediately upon opening the sample flask (1st score). Then the sample is aerated by vigorously shaking the open flask, and the second assessment is carried out (2nd score). The results of each panel experts were protocoled with a gradation of plastic odors according to a 7-point scale, where 1 point is no odors (no difference between the sample flask and empty one) and 7 points is a strong odor (obvious and significant differences between the flask and empty one). The 1st and 2nd scores are taken as the arithmetic mean of the odor intensity for each test separately obtained from 6 experts. If the scores were contrary, the procedure of the assessments was repeated.

2.3. Multisensor chip

In this study, we utilized a multielectroded chip, made of a thermally oxidized Si wafer. The chip size is 10 × 10 mm^2. SiO_2 layer thickness is about 300 nm. On the top of this layer, we realized 18 strip co-planar

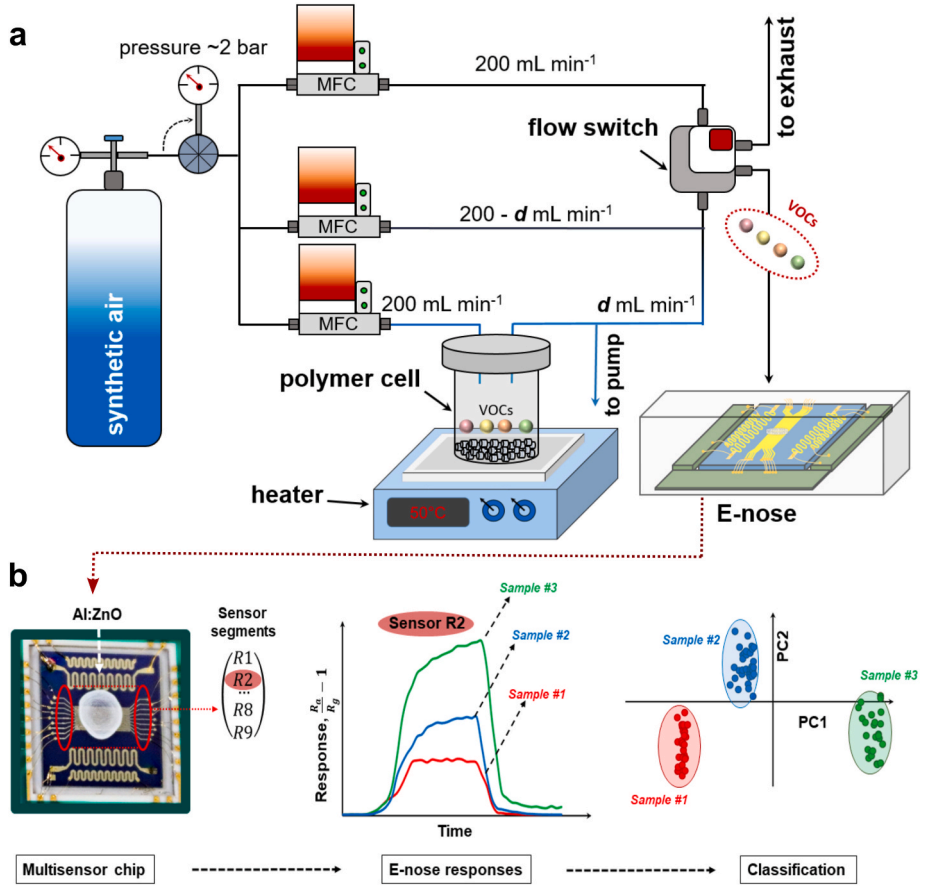

Fig. 1. Design of a setup for estimating the food plastic odors using an *Al-doped ZnO*-based electronic nose: (**a**) scheme of a gas-analytical system; (**b**) illustration of the sensor chip operation when exposed to organic impurities from the polymer granules with further classification of the responses by pattern recognition methods.

electrodes to be covered with an *Al-doped ZnO* sensing layer, two meander thermoresistors, and two meander heaters to control the temperature (Fig. 1). The electrodes are made of Pt (150 nm) on Ti adhesive layer (5 nm) using magnetron sputtering. Each pair of electrodes is distanced by 50 μm and can be regarded as a sensor, or a sensor segment of the multisensor chip. The chip temperature was calibrated with an IR pyrometer Kelvin Compact 1200D (*"Euromix" CJSC*, Russia) and maintained with an accuracy of ±5 °C. Prior to the measurements, we stabilized the chip at 300 °C for 24 h.

The chip was installed into a ceramic card which was connected to an electric board to control the temperature and record sensor segments' resistance. Our pre-experimental tests suggested the optimum temperature to be 250 °C. All the data are given for the chip with 9 operating segments.

2.4. Gas-mixing setup and sensor performance

The chip performance was evaluated in a chamber, 0.76 cm^3, where a stable flow of 200 sccm was maintained. We supplied synthetic air at (23 ± 0.5) °C from the pure air source. The synthetic air was forwarded into two lines passing mass flow controllers, MFCs (*Bronkhorst®*, the Netherlands), as shown in Fig. 1a. The first line was used to measure the sensors' resistance in the base atmosphere, i.e., contained only synthetic air. The other line ensured the measurements of the polymer odors. A weighted amount of polymer granules ($m \approx 15\,g$) was placed in a steel container, which is incorporated in this line, with a disposable aluminum crucible. The temperature of the container was controlled by a heater with feedback managed by means of a thermocouple placed inside the container. An airflow of 200 sccm was passing through the chamber with a polymer sample in all experiments. At high temperatures, polymers tend to emit smells rather intensively which might result in exceeding our electric board's measurable range of resistance. In order to decrease the vapor concentration, we diluted it by the synthetic air flow using the third line. As two lines provide the total flow of 200 sccm passing through the chamber with e-nose, we diluted the vapor concentration by a factor of 4 times at 50 °C and by a factor of 20 for 75 °C pumping out a part of the flow passed through the chamber. The pumped-out flow was compensated by the air from the third line. Finally, the lines were forked using an automatic switch valve to be forwarded either to a chamber with the chip or to the exhaust.

Our protocol included exposure of the chip for 20 min to the synthetic air, then to air passed through the polymer granules for 2 min and then switching the flow to the synthetic air for 4 min. The time of exposure of the chip to the synthetic air of 20 min was chosen as an optimal one from two points of view: first, for ensured the removal of residual volatiles left from the previous test, i.e., the plastic samples have different VOC content and, as a consequence, the different recovery times of sensor response to the pre-test values; second, to reach the solid phase/gas phase equilibrium for the new sample in the test cell under dynamic conditions.

For the description of sensing performance, we calculate the chemiresistive response, *S*, facilitated by the appearance of vapors in the air:

$$S = f \cdot \Delta R \,/\, R_{sample}, \tag{1}$$

where R_{sample} [MΩ] is the average resistance of the sensor segments in the polymer-related VOCs atmosphere and ΔR [MΩ] $= R_{air} - R_{sample}$ represents the change in the resistance due to the difference in polymer-related VOCs resistance (R_{sample}) and average resistance in the background air (R_{air}), *f* is a dilution coefficient, equaled 0.05, 0.2 and 1.0 for the temperatures 75, 50 and 25 °C, accordingly. The average resistance values of the sensor segments were collected from the last 10 and 100 points before changing the type of atmosphere for R_{sample} and R_{air}, respectively, provided that the relative standard deviation s_r of the studied point sampling was no more than 5%, i.e., when resistance values are stabilized due to saturation at a given concentration of volatile vapors. If this value was higher, then the point sampling was reduced until the desired s_r value was obtained. For a clear representation of the resistance transients, we use the normalized resistance, which is the segment resistance divided by R_{air} (Fig. 1b).

As an alternative method for the analysis of polymer odor profiles, we used a mass spectrometer with a quadrupole mass analyzer *Universal Gas Analyzer UGA-100* (*SRS*, USA). The mass spectrometric analysis was carried out simultaneously with e-nose tests/data acquisition.

2.5. Data analysis

To analyze and classify the multivariate data ($n = 9$) of sensor responses to VOCs from the polymers, we applied pattern recognition approaches, such as principal component analysis (PCA) and linear discriminant analysis (LDA), and *Random Forest* algorithm.

PCA is a statistical method to reduce the dimensionality of data (Jackson, 1991). The calculation of the principal components can be reduced to the singular value decomposition of the data matrix, or to the eigenvectors and eigenvalues of the covariance matrix of the original data (Tharwat, 2016). The approach allows one to discard less significant features in sensor responses by directing the axes of the principal components along the maximum scatter of the data variance. Thus, it helps to display the space of high metrics in the Cartesian coordinate system. However, PCA does not provide a predictive estimate for closely spaced clusters of response data. For a comparative evaluation of this approach and data processing protocols with the preliminary training, we employed the supervised methods of linear discriminant analysis (LDA) and *Random Forest* machine learning algorithm.

LDA is a generalization of Fisher's linear discriminant (Fisher, 1936) to find a linear combination of features that describes or separates two or more classes (Izenman, 2013; Tharwat et al., 2017). The resulting combination can be used as a linear classifier, or, more commonly, for dimension reduction before the classification. The second approach is a machine learning algorithm based on the *Decision Tree* model. The main idea is to use a large ensemble of decision trees; each tree gives a not good quality of classification, but due to their large number, the accuracy result gets better (Breiman, 2001; Breiman et al., 1984).

Thus, in order to classify the obtained data, the PCA and LDA approaches were compared for the dimension reduction and data clustering, and then we applied the *Random Forest* classification algorithm for the plastics recognition. The models of the *PCA* and *LinearDisciminantAnalysis* classifiers and the *RandomForestClassifier* machine learning protocol were implemented from the *Scikit-learn Python* package (*version 1.0.2*) with default settings (Pedregosa et al., 2011; Raschka, 2015). For the classification algorithm, sensor response data for 3 types of plastics and synthetic air were used, and this data has been divided into train and test datasets in a ratio of 0.35–0.65, respectively. The selection of optimal parameters for obtaining high accuracy of plastics recognition in a multidimensional response space was carried out using the *GridSearchCV* package of the *Scikit-learn* software library.

2.6. Correlation and regression "Al-doped ZnO e-nose vs sensory evaluation"

To estimate the ability of the *Al-doped ZnO* e-nose to predict the sensory characteristic of primary and secondary polymers we additionally analyzed their possible relation. We collected the chemiresistive responses data for the 17 food plastics and polymer compounding products using an *Al-doped ZnO* e-nose based on an array of 11 sensors. For each of the studied polymers, we also obtained sensory evaluation scores from the expert panel. A full list of polymer samples with a two-score sensory assessment is presented in Table S1. To access the correlation between the sensory evaluation scores and the e-nose segment responses we apply Pearson's correlation coefficient *r*:

$$r = \frac{\sum_{i=1}^{17}(x_i - \overline{x})(y_i - \overline{y})}{16 \bullet s_x \bullet s_y}, \quad (2)$$

where x_i, y_i – variables of the samples (11 sensor segments, *R1-R11*, and 2 sensory evaluation scores); $\overline{x}, \overline{y}$ – the mean values of the variables for the samples of 20; s_x, s_y – standard deviation for the samples. For such sampling size, a strong positive or strong negative correlation is observed if the correlation coefficient is more than a critical value r_{crit} of 0.606 ($p = 0.01, n = 17$) (Aspelmeier, 2005).

Assuming a correlation between the e-nose performance and sensory evaluation scores, we applied the multiple linear regression models for defining the patterns between the responses of the *Al-doped ZnO* e-nose, as independent variables or *predictors*, and sensory evaluation scores, as dependent ones. The data were analyzed using *IBM SPSS Statistics-version 28* (IBM Corp. Released, 2021. IBM SPSS Statistics for Windows, Version 28.0. Armonk, NY: IBM Corp.). The algorithm of fitting the data by the best model is based on the gradual removal of the independent variables with the low Pearson's coefficient *r*. The results of such data dimensionality decrease were evaluated by comparing the adjusted R^2.

We built regression models for the first and second sensory evaluation ratings. As an assessment of the quality of the proposed model, the coefficients of determination R^2 were calculated (Table S2). According to the data on Pearson's correlation coefficients, we evaluate the quality of the correlation when using the method of backward elimination of predictors that have a poorly pronounced correlation with the dependent variables of the regression model. Thus, we studied regression models for the first and second sensory evaluation scores with e-nose responses using the full and eliminated set of predictors (Table S3).

3. Results and discussion

3.1. Physical and chemical features of HDPE-based plastics

We studied polymers based on high density polyethylene (HDPE), which is a high molecular weight organic compound with a single carbon–carbon $–CH_2–CH_2–$ bond between units and low numbers of terminal $–CH_3$ groups per 1000 carbon atoms. These compounds are high-carbon analogs of alkanes obtained by the ethylene polymerization reaction with an almost unbranched linear structure and a high degree of crystallinity. The appearance of the samples, all made of HDPE, is given in Fig. 2a (insets): a primary polymer (*Sample #1*), recycled polymers with (*Sample #2*) and without (*Sample #3*) the zeolite adsorbent additive used to remove odors after recycling processes. To evaluate the differences in vapor appearance and temperature of polymers' degradation in air, we carried out STA-MS and gravimetric tests (see Fig. 2a and Table S4 in the Supplementary Materials). We monitored the processes occurring at the time of thermal degradation of polymers due to changes in the polymer mass and intensities in the DSC function (μV/mg) as well as in the values of the ion current at $m/z = 44$ (characteristic molecular ion CO_2^+ during the degradation of hydrocarbon polymers). The STA-MS data for the polymers suggest a decrease of the DSC function in the temperature range of 120–125 °C, which corresponds to the melting point of high-density polyethylene and, accordingly, the polymer transition to a viscous-flow state. For the primary polymer, intense degradation processes in the temperature range of 430–440 °C are presumably associated with the breaking of the carbon-carbon bonds (Norris, 1932), due to the presence of narrow intense peaks of DSC and ion current. Similar peak positions for DSC and ion current are observed for recycled plastic samples, which confirms the assumption of oxidative degradation of polymers. However, for recycled samples, there is also an increase in heat flux and ion current at higher temperatures (T > 450 °C), which might hint at the presence of organic impurities in these samples, which can be associated with the presence of odors of these plastics. Gravimetric tests were carried out to estimate the content of

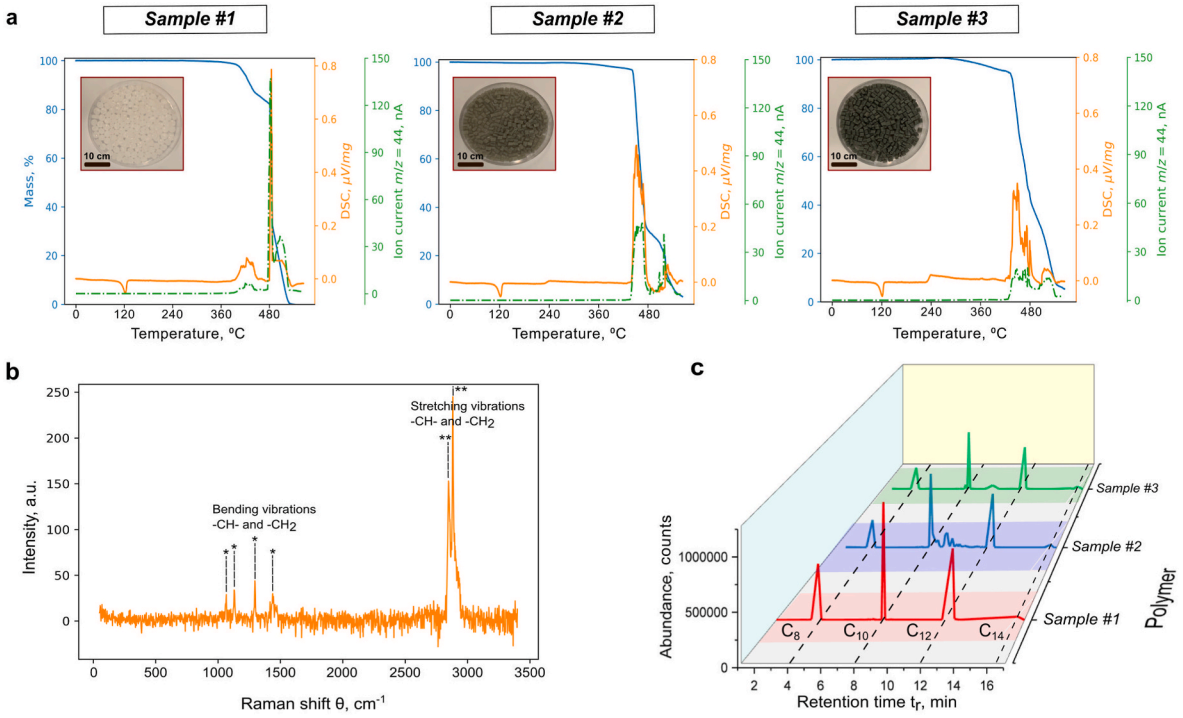

Fig. 2. Physicochemical characteristics of the polymer samples: (**a**) TGA/DSC-MS analysis for plastic samples; (**b**) Raman spectroscopy of the polymer's structure for *Sample #1*; (**c**) Qualitative Headspace-GC-MS analysis of polymer samples with a semi-quantitative evaluation of volatile compounds (T = 70 °C; signal-to-noise ratio - 1489:1).

VOCs in polymer granules when heated to temperatures 50, 75, and 105 °C. The choice of temperatures for the gravimetric assessment of VOCs content and its further evaluation by *Al-doped ZnO* e-nose was made with an attempt to reduce the time for reaching the subsequent thermal equilibrium of polymer samples when compared to the standard procedures for determining the VOCs content in polymer matrices (*ASTM D 4526-96:2001 Standard Practice for Determination of Volatiles in Polymers by Static Headspace Gas Chromatography* (2001), *ISO 13741-1:1998 Plastics/rubber — Polymer dispersions and rubber latices (natural and synthetic) — Determination of residual monomers and other organic components by capillary-column gas chromatography*, 1998). The VOC content is significantly different for polymers after the annealing at the temperature of 105 °C (Table S4 in the Supplementary Materials). The relative VOC contents of *Sample #1*, *Sample #2* and *Sample #3* at 105 °C are correspondingly 0.23 ± 0.05%, 0.22 ± 0.03% and 0.30 ± 0.04%. For *Samples #1* and *#2* these characteristics are similar due to the presence of a zeolite additive in *Sample #2*. According to this, the zeolite helps to enhance the adsorption of volatile substances which providing the shift of the e-nose vector signal to the one of the primary polymer (*Sample #1*) (Supplementary Materials).

The qualitative assessment of the structure of plastic, *Sample #1*, by Raman spectroscopy indicates high density polyethylene (Fig. 2b) (Araujo et al., 2018; Mutter et al., 1993). The peaks at 1430-1470 cm^{-1} and 2840-2900 cm^{-1} respectively correspond to the bending and stretching vibrations of the –C–H and $–CH_2$ bonds in the alkane chain. For recycled polymers, a wide blurring of vibrational reflections in the spectra is observed, which is likely due to the high content of impurities in the composition. Additionally, we assess the similarity of the structure of samples to standard high density polyethylene by FT-IR spectroscopy (Fig. S2). The high-intensity peaks at 2914 cm^{-1} and 2846 cm^{-1} are asymmetric and symmetric stretching vibrations $–CH_2–$, respectively. The peaks at 1472 cm^{-1}, 1464 cm^{-1} are related to deformation vibrations $–CH_3$, $–CH_2–$. Bands 730-720 cm^{-1} refer to deformation oscillations $–CH_2–$. Moreover, we observe that the intensity of ATR pikes for secondary polymer samples (*Sample #2* and *Sample #3*) is higher than for primary polymer (*Sample #1*). This effect can be related to the lower concentration of the preliminary$–CH_2–CH_2–$ bond monomer units in the secondary polymers due to the defects and organic residuals arising during the polymer use, which also can be supported by the differences of ion currents in STA-MS tests, particularly the ion current values for *Sample #1* is higher than *Sample #2* and *Sample #3*.

To confirm the stated hypotheses, we carried out a headspace GC-MS analysis of the plastic samples. The results of the analysis are presented in Fig. 2c and Table S5. We found that the volatile compounds from the gas phase of the studied polymers represent a mixture of non-polymerized high-carbon *n*-alkanes, primarily, octane C_8H_{18}, decane $C_{10}H_{22}$, dodecane $C_{12}H_{26}$, and tetradecane $C_{14}H_{30}$, with a total share above 95%, 50% and 83% for *Sample #1*, *Sample #*2 and *Sample #*3, respectively. Thereby the content of unidentified components and impurities in samples of recycled polymers is more than 15%. This number of unidentified components indicates the need for accurate control of the secondary polymer composition to ensure a high degree of recycling quality before implementing the plastics for further applications.

Comprehensive analysis of polymer products using STA-MS, optical methods (Raman and IR spectroscopy), as well as gas chromatography with various detection options, confirms critical differences in the degree of suitability of plastics as materials for further applications. Although these approaches might help to evaluate the particular polymer or VOCs associated with it, they are most often costly in terms of equipment energy supply, expensiveness, and express quality assessment, especially for the purpose of controlling recycling processes in production.

3.2. Application of E-nose based on Al-doped ZnO for plastic odor analysis

We further analyzed the polymer samples using an on-chip made multisensor array with a sensitive *Al-doped ZnO* layer. The odor profile of plastics is a mixture of VOCs, just as shown earlier, that facilitates a unique response of sensor segments. We compared the odor profiles of the samples acquired at 25 °C with the profiles obtained when the polymers were heated to 50 °C and 75 °C to intensify the desorption of volatile compounds from the polymer surface. We recorded the data of four repeated cycles for each of the polymers at different temperatures. When the chip is exposed to air with organic vapors, we observed a change in the analytical signal of the multisensor chip, i.e., chemiresistive responses of the sensor segments (Fig. S3 in the Supplementary Materials), regardless of the sample temperature. However, as the polymer sample temperature rises, an increase in the chemoresistive response is observed, which is associated with the gradual desorption of VOCs and solvent residuals from the plastic surface and, as a result, an increase in the concentration of volatile substances. Also, the relative standard deviations (s_r) under different conditions for *Sample #1*, *Sample #2,* and *Sample #3* are presented in Table 1 and Fig. S3 in the Supplementary Materials. Thus, we found that the recycled polymer sample (*Sample #3*) has the lowest RSD value, which contributes to the good achieved reproducibility for the analysis of secondary polymers. This may be due to the presence of a high concentration of volatile compounds, in contrast to *Sample #1* and *Sample #2*. High RSD values at 25 °C compared to similar values at elevated temperatures are likely due to the weak desorption of VOCs from the surface of the polymer granules, which leads to more pronounced differences in parallel tests for the identical polymer samples. According to this, a large data scatter is also observed at the low sample temperature, which indicates that a proper polymer quality analysis should be carried out at 50 °C.

Under the supply of synthetic air, containing VOCs desorbed from the surface of the studied samples, the resistance of the *Al-doped ZnO* sensor segments decreases, which indicates the *n*-type sensor response (Fig. 3a). This is because the VOCs are the reducing ones ("electron donors") as the presence of high-carbon alkanes was established by headspace GC-MS results, and thus we observe the increase of conductivity of these *n*-type semiconductor sensor segments by exposure to VOCs. The mean response values ($\overline{R}$) for *Sample #1*, *Sample #2*, and *Sample #3* are described in Table 1 and Fig. 3b). The shown unique combination of sensor responses is the so-called 'fingerprints' of plastic in the artificial space of perception of plastic odors by an electronic nose. We collected a database of fingerprints for each type of polymer at the explored heating temperatures. It was found that with an increase in the sampling temperature, there was an increase in the chemiresistive response of the electronic nose sensor segments due to the higher concentration of volatile compounds in the synthetic air flow. However, comparing the average response rates at elevated temperatures, we observe that for a sample with an adsorbent additive in a polymer composite, lower chemiresistive responses are detected than for another recycled plastic. This effect can be related to the high adsorption

Table 1
Sensing characteristics of *Al-doped ZnO*-based electronic nose to the plastic samples.

Temperature, °C	*Sample #1, %*		*Sample #2, %*		*Sample #3, %*	
	$\overline{R}$	s_r, %	$\overline{R}$	s_r, %	$\overline{R}$	s_r, %
25	0.008 ± 0.002	*17*	0.05 ± 0.01	*13*	0.46 ± 0.04	*10*
50	0.041 ± 0.003	*1*	0.14 ± 0.01	*7*	0.83 ± 0.04	*2*
75	0.035 ± 0.002	*9*	0.12 ± 0.02	*10*	0.78 ± 0.02	*3*

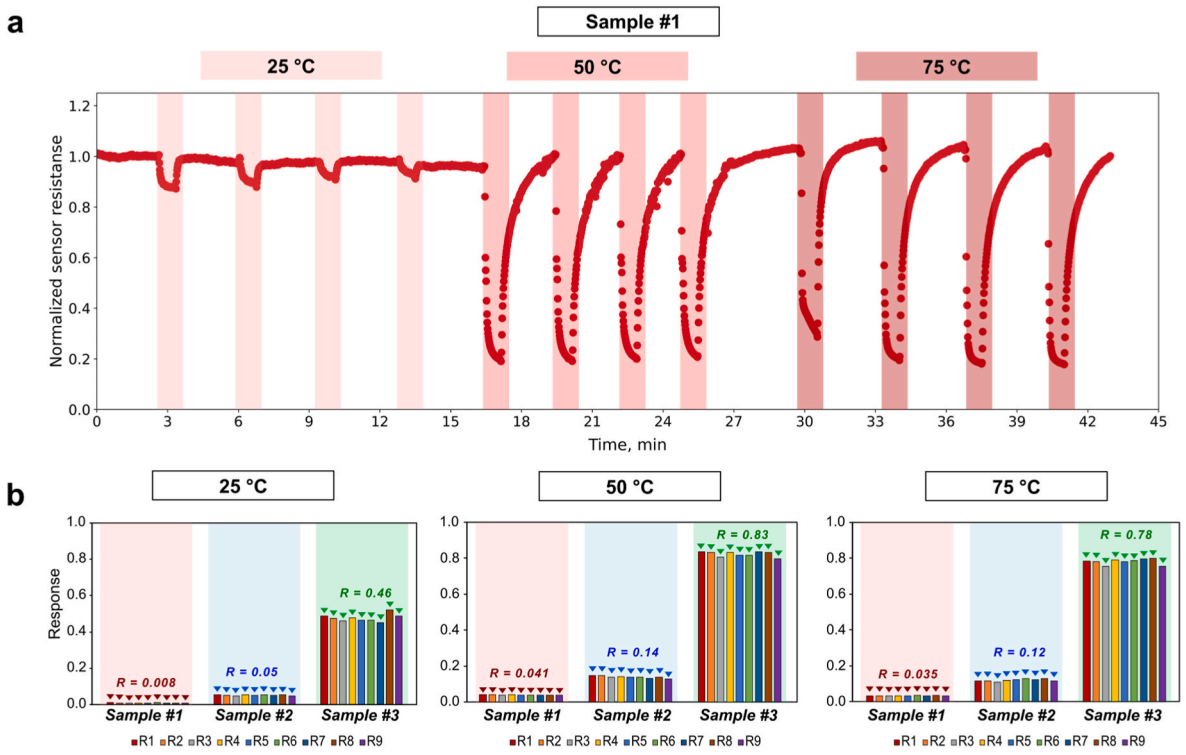

Fig. 3. Analysis of polymer samples using an *Al-doped ZnO*-**based electronic nose:** (**a**) the plastic odor analysis for *Sample #1*: sensor responses of the electronic nose to VOCs in the air at 25 °C and heated to 50 °C and 75 °C, and (**b**) obtained polymers odor "fingerprints". R1 – R9 – the sensor segments at the chip. (*Sample #1* at υ_{flow} = 200 sccm; *Sample #2* at υ_{flow} = 50 sccm (total flow: 200 sccm; dilution = *4:1*); *Sample #3* at υ_{flow} = 10 sccm (total flow: 200 sccm; dilution = *20:1*)).

capacity of the additive with respect to organic substances on the polymer surface. The detailed assessment of the influence of zeolite additives on the chemiresistive responses is presented in **Note #1** and Fig. S4 in the Supplementary Materials.

A comparison of the results obtained by *Al-doped ZnO* e-nose and alternative methods such as GC-MS, STA-MS, FT-IR spectroscopy, and gravimetry indicates that residual organic substances appeared due to polymer recycling contribute more significantly to the e-nose responses when compared residual monomers (octane C_8H_{18}, decane $C_{10}H_{22}$, dodecane $C_{12}H_{26}$, and tetradecane $C_{14}H_{30}$). In particular, this assumption is confirmed by the observed changes in the ion current values for $m/z = 44$ when conducting STA-MS tests and the decrease in the intensity of the main peaks (2914 cm^{-1} and 2846 cm^{-1}) at FT-IR spectra for the secondary polymers in comparison with the primary one.

Also comparing the results obtained with the *Al-doped ZnO*-based electronic nose at 25 °C conditions and the results of the sensory evaluation of the expert panel (Table S6 in the Supplementary Materials), we observe that the higher the mean response value of the e-nose, the higher the score given by the expert panel. At the same time, for *Sample #2* with the addition of a zeolite adsorbent, the score of the expert panel turned out to be lower than for a similar polymer without this additive (*Sample #3*), which confirms our suggestion about the odor absorption by a zeolite. This fact is also reflected in the lower value of the mean e-nose response for *Sample #2* when compared to *Sample #3*. Thus, we can conclude that the scores of the expert panel coincide well with the e-nose analytical signals.

Simultaneously with the measurements by an electronic nose, we performed a mass spectrometric analysis of the gas phase containing volatile components from polymers (Fig. S5). At 25 °C, a similar ratio of the intensities of the gas phase components was observed, as in the case of the sensor responses of the electronic nose. For recycled polymers, peak intensity is observed for $m/z = 18$ and 36, which is most likely due to the presence of various oxidized carbon-containing compounds and possibly residual adsorbed water molecules. With an increase in the plastic sample temperature, the number of significant peaks decreases to determine the expected composition of a mixture of volatile substances. Increasing the polymer heating temperature, in the case of an alternative method of polymer quality testing (mass spectrometry), makes the task of accurate and error-free classification of samples difficult to achieve. However, the e-nose fingerprints of polymers at any studied temperature provide more precise characteristics for classifying plastics according to their quality in the space of sensor segment components.

3.3. Machine learning and classifiers protocols for plastics recognition

Each fingerprint is a multi-dimensional array of responses (or resistances) associated with a particular plastic. Thus, this characteristic can be considered as the coordinates of the radius-vector in the multi-dimensional space of responses (in our case, the 9-dimensional one). To display such a set of characteristic vectors in the 2D space of the Cartesian system, it is necessary to reduce the dimension of the space by extracting the principal components (PCs) or a combination of eigenvectors (LDA, an algorithm similar to Fisher's linear discriminant (Fisher, 1936)) with a minimum loss in the accuracy of the relative arrangement of clusters. In the PCA method (unsupervised) (Tharwat, 2016), the search for new components, in the space in which a set of plastic fingerprints are classified, is determined by finding an orthogonal transformation for which the sample variance S_m^2 for m different fingerprints x_i along the direction specified by the normalized vector a_k would be maximum:

$$S_m^2[(X, a_k)] = \frac{1}{m}\sum_{i=1}^{m}(a_k, x_i)^2 = \frac{1}{m}\sum_{i=1}^{m}\left(\sum_{j=1}^{n} x_{ij}, a_{kj}\right)^2 \rightarrow max. \quad (3)$$

Thus, such subspaces are sought, in the projection on which the standard deviation between adjacent patterns would be maximum, thereby

determining the maximum degree of data resolution in space with minimal distortion of the original datasets.

The algorithm of linear discriminant analysis (supervised) also allows reducing the multidimensionality by finding eigenvectors, which can be used to select the necessary features to improve the accuracy of classifying points in a new space (Tharwat et al., 2017). Using the statistical considerations outlined in these two approaches, we applied them to the dataset obtained by the electronic nose. Fig. S6 shows the possibility of space dimension reduction for raw data of plastic fingerprints depending on the sample temperature. Based on the obtained data, several features were observed. Firstly, for all cases, the proportion of explained variance exceeds 99.0%, which indicates a qualitative assessment of this classification using one PC1 or LD1 component. Secondly, from the classification data, we found out that in the case of the temperature of 25 °C (Figs. S6a and d) there is an overlap of fingerprint clusters related to *Sample #1*, *Sample #2,* and synthetic air. This fact can be explained by the presence of an absorbent additive in the composition of *Sample #2*, which reduces the intensity of the sensor signal to a level comparable to that of primary plastic as well as the non-odor gas profile of Sample #1 which makes it similar to synthetic air cluster. At a temperature of 50 °C (Figs. S6b and e), an overlap of fingerprints related to polymer samples and synthetic air is not observed due to active thermal desorption of VOCs from the polymer surface. With a further increase in temperature (Figs. S6c and f), better discrimination of plastics is visually detected, i.e., the larger projection of the distance between the centroids of the three classes when compared to the 25 °C clustering; we conclude that the use of high-temperature annealing in the quality analysis process of plastics may lead to a decrease in the rate of false-positive classification results. Thus, the use of thermal desorption of components from the surface of polymers for further classification by quality is rather effective, particularly due to the competitive gas adsorption and change of component's vapor pressure.

To selectively classify polymers based on their odor profiles and confirm the assumption about the effect of temperature exposure on the composition of plastic odor profiles, the *RandomForestClassifier* machine learning algorithm was used with the selection of 7 optimal classifier parameters using the *GridSearchCV* package. The results of data classification using this protocol are presented in Table S7 (Supplementary Materials). This model works according to the *DecisionTree* protocol, the main ideas of which were outlined in the works of the mathematician L. Breiman (Breiman, 2001; Breiman et al., 1984), that is, thanks to a number of "*voting*" classifier trees.

Fig. 4 and Fig. S7 in the Supplementary Materials show plots with decision boundaries regarding the pairwise distribution of plastic fingerprint data and confusion matrices at optimal parameters. A choice of pairwise representation is for simplicity only, but the classification is made for the odors from all samples and pure air. The accuracy of the proposed approach at temperatures of 25, 50, and 75 °C was 98.5%, 100.0%, and 99.9%, respectively (see Table S7 in the Supplementary Materials), as well as there is also an increase in differences between sensor responses for the primary and secondary polymers, which enhances the quality of the analysis, especially at elevated temperatures. As expected from the results of principal component analysis and linear discriminant analysis, the minimum value of the pairwise resolution coefficient of *plastic_1/plastic_2* or *synthetic air* is observed at 25 °C and increases with increasing temperature, which makes it preferable to carry out the analysis under the elevated conditions and to enhance the

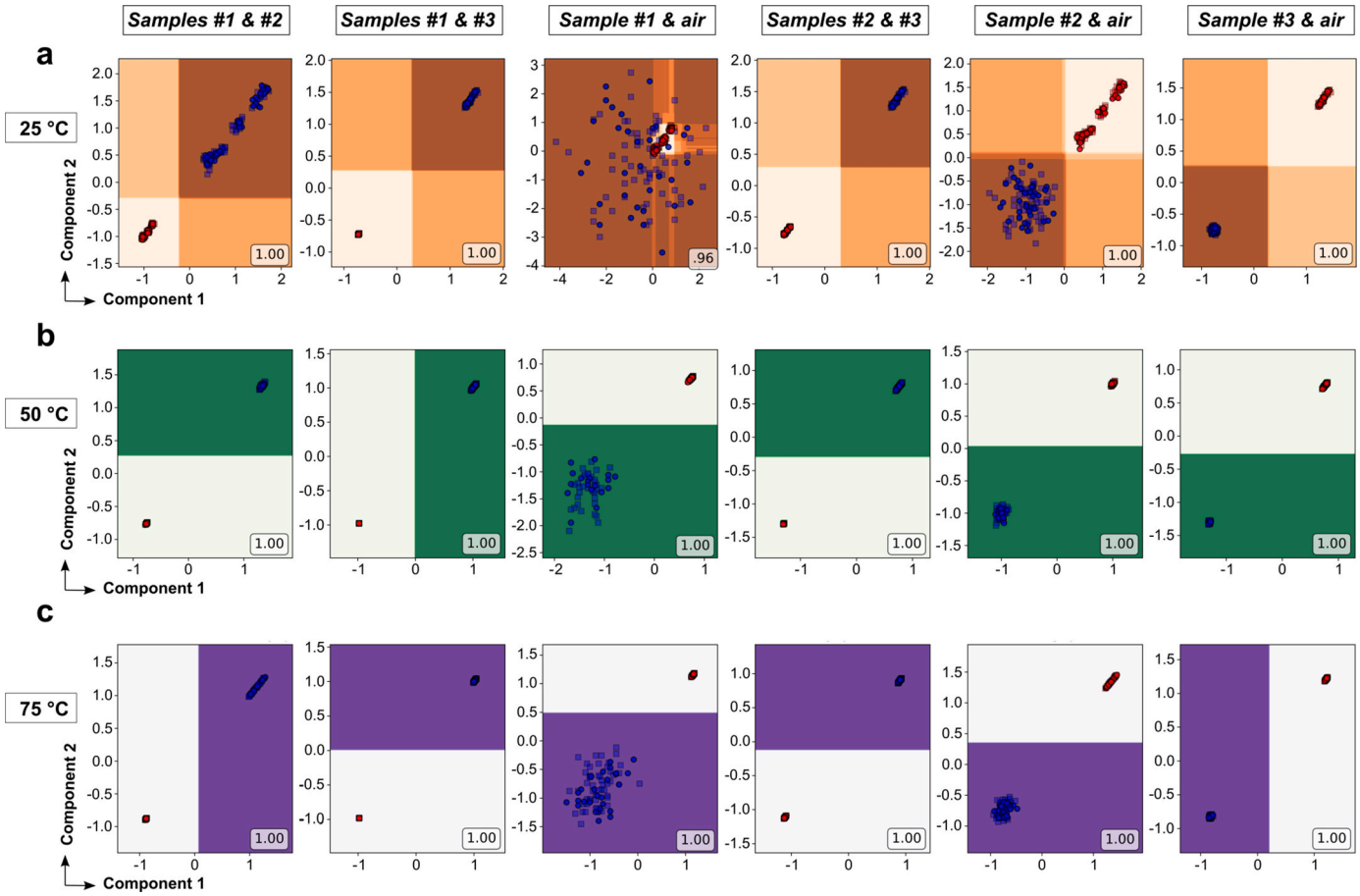

Fig. 4. *Random Forest* algorithm for the plastics recognition by classifying e-nose data: accuracy of pairwise recognition of 3 polymers and synthetic air at the different sample temperatures: **a)** T = 25 °C; **b)** T = 50 °C; **c)** T = 75 °C.

accuracy and objectivity of analysis.

Thus, the proposed approach of combining an electronic nose based on the *Al-doped ZnO* sensitive layer with machine learning protocols with the additional thermal impact on plastics makes conditions for an express qualitative assessment of the state of plastic recycling in comparison with the virgin samples and enables selective recognition of the primary and secondary polymers.

3.4. Correlation of the e-nose responses and sensory analysis

Based on the data comparing the sensory assessment by the expert panel (Table S6) and the e-nose responses (Table 1), we notice a pronounced relationship between the odors of polymers assessed by sensory analysis and chemoresistive responses, allowing us to hypothesize a possible good correlation.

To check the proposed hypothesis, we tested 17 various food plastics and polymer compounding products based on polymer matrices such as high density polyethylene (**HDPE**), polypropylene (**PP**), and polyethylene terephthalate (**PET**) (Table S1) by sensory evaluation technique and using an 11-segment multisensor array based on *Al-doped ZnO* similar to what we used in previous tests. A positive relationship between the predictors and variables is clearly expressed (Fig. 5a and b). We calculated Pearson's pairwise correlation coefficients (Benesty et al., 2009) for the obtained data. The correlation coefficients for most of the chemoresistive responses (*predictors*) with sensory evaluations (*dependent variables*), except for the R11 sensor segment, exceed the critical value of Pearson's coefficient for a given sample size of polymer samples. Still, using Pearson's correlation coefficient, it is only possible to determine the pairwise linear interrelation between the predictor and dependent variable. So, the relation between the full set of predictors and dependent variables was evaluated by regression analysis methods.

We built a mathematical model, multiple linear regression (Baskar et al., 2017; Sipos et al., 2011), that establishes dependence between a predictor and dependent variable, i.e. the e-nose responses and sensory evaluation scores:

$$F = \sum_{i=1}^{11} \beta_i R_i + c, \tag{4}$$

where F – a value of sensory evaluation score (dependent variable); β_i– regression coefficient; R_i – chemiresistive response of sensor segment with the number i (predictor); c - error terms or constant value. Due to the multidimensionality of the studied data, we applied the expected versus observed cumulative probability plots (Fig. 5c and d) of the regression standardized residuals for the clear representation of the regression model.

We observed that the resulting models have R^2 coefficients above 0.975, which indicates the high quality of the constructed models (Table S2 in the Supplementary Materials). Moreover, the exclusion of the predictors R5, R11, and R1, R11 for models with the first and second sensory assessments, respectively, did not lead to a significant increase in the R^2 coefficient. However, it is worth noting that the model based on the second sensory assessment gives slightly higher regression quality values than the model for the first one, which is presumably due to the greater similarity of the second sensory evaluation procedure to the e-nose measurements.

4. Conclusion

We demonstrated a rapid and accurate approach to determine the quality of high-density polyethylene compounds as well as the effect of zeolite adsorbent additive on the plastic odors using an Al-doped zinc oxide based electronic nose and machine learning tool. PCA and LDA clustering were implemented for the polymer discrimination in 2D component space at different sample temperatures. We found that the higher the sample temperature, the higher the effect of the zeolite additive on the odor profile of the recycled polymer, and the better cluster discrimination and reproducibility. Using the *Random Forest* machine learning classifier, we observed that the pairwise discrimination ratio of plastics in the fingerprint space was more than 98.5%, which showed a

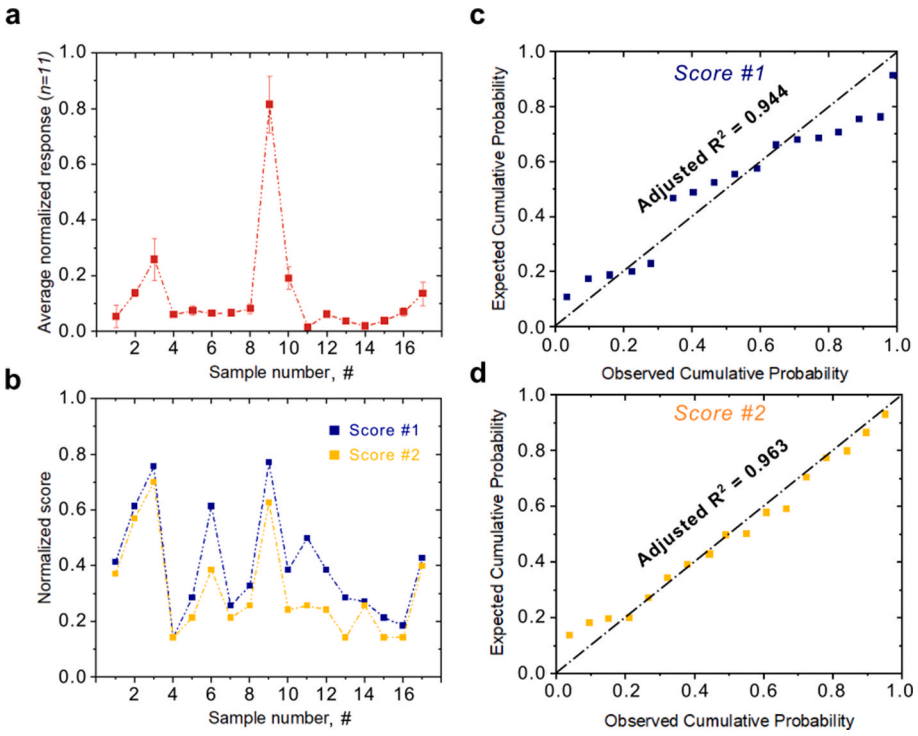

Fig. 5. Correlation assessment and regression model between the *Al-doped ZnO* e-nose based on the array of 11 sensors and two-score sensory evaluation: (**a**) average normalized responses of 17 polymers; (**b**) normalized sensory evaluation scores; (**c, d**) Expected *versus* observed cumulative probability plot of the residuals in the regression models.

high resolution between the average response data of the row-vectors in the range from 0.8% to 46%, from 4% to 83% and from 3.5% to 78% at 25, 50 and 75 °C, respectively. The differential scanning calorimetry approach with mass spectrometric detection (STA-MS), headspace GC-MS, Raman, and FT-IR spectroscopy were implemented as alternative methods for analyzing the structure and properties, which confirm the correlation between sensor responses and sensory characteristics of plastics. We also achieve a good positive correlation between the sensory features of studied polymers and *Al-doped ZnO* e-nose responses, which helps to involve the multiple linear regression model with the R^2 coefficient of more than 0.975. According to the analytical characteristics, compactness, and artificial intelligence tools, we believe that the proposed smart multisensor systemis a promising approach for assessing the quality of plastics in the production processes for food and pharmaceutical industries.

CRediT authorship contribution statement

Valeriy Zaytsev: Conceptualization, Methodology, Validation, Investigation, Writing – original draft. **Fedor S. Fedorov:** Conceptualization, Methodology, Investigation, Writing – original draft. **Boris Goikhman:** Conceptualization, Methodology, Formal analysis, Data curation. **Alexander Maslennikov:** Validation, Formal analysis, Visualization. **Vasilii Mashukov:** Supervision, Project administration, Funding acquisition, Resources. **Nikolay P. Simonenko:** Methodology, Resources. **Tatiana L. Simonenko:** Investigation, Methodology. **Dinara Gabdullina:** Validation, Project administration, Resources. **Olga Kovalenko:** Validation, Resources. **Elizaveta P. Simonenko:** Supervision. **Polina Kvitko:** Investigation, Methodology. **Olga Penkova:** Investigation, Methodology. **Dina Satybaldina:** Formal analysis, Data curation, Writing – review & editing. **Shakhmaran Seilov:** Project administration, Funding acquisition. **Tatiana S. Dubinina:** Investigation, Formal analysis, Data curation. **Dmitry A. Gorin:** Supervision, Writing – review & editing. **Albert G. Nasibulin:** Supervision, Project administration, Funding acquisition, Writing – review & editing.

Declaration of competing interest

The authors declare that they have no known competing financial interests or personal relationships that could have appeared to influence the work reported in this paper.

Data availability

Data will be made available on request.

Acknowledgment

The authors thank Dr. Vladislav Kondrashov and Mr. Andrei Starkov for their contribution to making a gas mixing system and express a deep gratitude to Mrs. Irina Belikova and Mrs. Evgenia F. Guschina for their valuable comments. This research was supported by the grant of the Russian Science Foundation № 21-73-10288, https://rscf.ru/en/project/21-73-10288 in the part of material synthesis, characterization, sensing performance evaluation, and machine learning. D.S. and Sh.S. thank Science Committee of the Ministry of Science and Higher Education of the Republic of Kazakhstan (grant number № AP14872171) for support of this research in part of regression model description. The authors thank the Council on grants of the Russian Federation (grant number НШ-1330.2022.1.3).

Appendix A. Supplementary data

Supplementary data to this article can be found online at https://doi.org/10.1016/j.jclepro.2023.138042.

References

Araujo, C.F., Nolasco, M.M., Ribeiro, A.M.P., Ribeiro-Claro, P.J.A., 2018. Identification of microplastics using Raman spectroscopy: latest developments and future prospects. Water Res. 142, 426–440. https://doi.org/10.1016/j.watres.2018.05.060.

Aspelmeier, J., 2005. Table of critical values for Pearson's r [WWW Document]. URL. https://pdf4pro.com/amp/view/table-of-critical-values-for-pearson-s-r-59198f.html.

ASTM D 4526-96:2001, 2001. Standard Practice for Determination of Volatiles in Polymers by Static Headspace Gas Chromatography.

Ball, P., 2020. The plastic legacy. Nat. Mater. 19, 938. https://doi.org/10.1038/s41563-020-0785-6.

Baskar, C., Nesakumar, N., Balaguru Rayappan, J.B., Doraipandian, M., 2017. A framework for analysing E-Nose data based on fuzzy set multiple linear regression: paddy quality assessment. Sensors Actuators A Phys 267, 200–209. https://doi.org/10.1016/j.sna.2017.10.020.

Benesty, J., Chen, J., Huang, Y., Cohen, I., 2009. In: Cohen, I., Huang, Y., Chen, J., Benesty, J. (Eds.), Pearson Correlation Coefficient BT - Noise Reduction in Speech Processing. Springer Berlin Heidelberg, Berlin, Heidelberg, pp. 1–4. https://doi.org/10.1007/978-3-642-00296-0_5.

Bigger, S.W., O'Connor, M.J., Scheirs, J., Janssens, J.L.G.M., Linssen, J.P.H., Legger-Huysman, A., 1996. Odor characterization of low-density polyethylene used for food-contact applications. In: Polymer Durability, Advances in Chemistry. American Chemical Society, pp. 17–249. https://doi.org/10.1021/ba-1996-0249.ch017.

Bo, R., Zhang, F., Bu, S., Nasiri, N., Di Bernardo, I., Tran-Phu, T., Shrestha, A., Chen, H., Taheri, M., Qi, S., Zhang, Y., Mulmudi, H.K., Lipton-Duffin, J., Gaspera, E. Della, Tricoli, A., 2020. One-step synthesis of porous transparent conductive oxides by hierarchical self-assembly of aluminum-doped ZnO nanoparticles. ACS Appl. Mater. Interfaces 12, 9589–9599. https://doi.org/10.1021/acsami.9b19423.

Breiman, L., 2001. Random forests. Mach. Learn. 45, 5–32. https://doi.org/10.1023/A:1010933404324.

Breiman, L., Freidman, J.H., Olshen, R.A., J, S.C., 1984. Classification and Regression Trees, first ed. Chapman & Hall/CRC, New York. https://doi.org/10.1201/9781315139470.

Buck, L., Axel, R., 1991. A novel multigene family may encode odorant receptors: a molecular basis for odor recognition. Cell 65, 175–187. https://doi.org/10.1016/0092-8674(91)90418-x.

Cabanes, A., Valdés, F.J., Fullana, A., 2020. A review on VOCs from recycled plastics. Sustain. Mater. Technol. 25, 1–22. https://doi.org/10.1016/j.susmat.2020.e00179.

Chae, Y., An, Y.-J., 2018. Current research trends on plastic pollution and ecological impacts on the soil ecosystem: a review. Environ. Pollut. 240, 387–395. https://doi.org/10.1016/j.envpol.2018.05.008.

Demets, R., Roosen, M., Vandermeersch, L., Ragaert, K., Walgraeve, C., De Meester, S., 2020. Development and application of an analytical method to quantify odour removal in plastic waste recycling processes. Resour. Conserv. Recycl. 161, 104907 https://doi.org/10.1016/j.resconrec.2020.104907.

Fedorov, F.S., Yaqin, A., Krasnikov, D.V., Kondrashov, V.A., Ovchinnikov, G., Kostyukevich, Y., Osipenko, S., Nasibulin, A.G., 2021. Detecting cooking state of grilled chicken by electronic nose and computer vision techniques. Food Chem. 345, 128747 https://doi.org/10.1016/j.foodchem.2020.128747.

Fedorov, F.S., Simonenko, N.P., Arsenov, P.V., Zaytsev, V., Simonenko, T.L., Goikhman, B.V., Volkov, I.A., Simonenko, E.P., Nasibulin, A.G., 2022. Study of programmed co-precipitation of aluminum doped zinc oxide for high precision design of gas analytical units. Appl. Surf. Sci. 606, 154717 https://doi.org/10.1016/j.apsusc.2022.154717.

Fisher, R.A., 1936. The use of MUultiple measurements in taxonomic problems. Ann. Eugen 7, 179–188. https://doi.org/10.1111/j.1469-1809.1936.tb02137.x.

Garcia, J.M., Robertson, M.L., 2017. The future of plastics recycling. Science 84 358, 870–872. https://doi.org/10.1126/science.aaq0324.

Gardner, J.W., Bartlett, P.N., 1994. A brief history of electronic noses. Sensor. Actuator. B Chem. 18, 210–211. https://doi.org/10.1016/0925-4005(94)87085-3.

Giron, N.H., Celina, M.C., 2017. High temperature polymer degradation: rapid IR flow-through method for volatile quantification. Polym. Degrad. Stabil. 145, 93–101. https://doi.org/10.1016/j.polymdegradstab.2017.05.013.

Goikhman, B.V., Fedorov, F.S., Simonenko, N.P., Simonenko, T.L., Fisenko, N.A., Dubinina, T.S., Ovchinnikov, G., Lantsberg, A.V., Lipatov, A., Simonenko, E.P., Nasibulin, A.G., 2022. Quantum of selectivity testing: detection of isomers and close homologs using an AZO based e-nose without a prior training. J. Mater. Chem. 10, 8413–8423. https://doi.org/10.1039/D1TA10589B.

Hahladakis, J.N., Velis, C.A., Weber, R., Iacovidou, E., Purnell, P., 2018. An overview of chemical additives present in plastics: migration, release, fate and environmental impact during their use, disposal and recycling. J. Hazard Mater. 344, 179–199. https://doi.org/10.1016/j.jhazmat.2017.10.014.

Han, J.-K., Kang, M., Jeong, J., Cho, I., Yu, J.-M., Yoon, K.-J., Park, I., Choi, Y.-K., 2022. Artificial olfactory neuron for an in-sensor neuromorphic nose. Adv. Sci., 2106017 https://doi.org/10.1002/advs.202106017.

Häußler, M., Eck, M., Rothauer, D., Mecking, S., 2021. Closed-loop recycling of polyethylene-like materials. Nature 590, 423–427. https://doi.org/10.1038/s41586-020-03149-9.

ISO 13741-1:1998 Plastics/rubber — Polymer Dispersions and Rubber Latices (Natural and Synthetic) — Determination of Residual Monomers and Other Organic Components by Capillary-Column Gas Chromatography, 1998.

ISO 3251:2019 Paints, Varnishes and Plastics — Determination of Non-volatile-matter Content, 2019.

ISO/DIS 5677 Testing and Characterization of Mechanically Recycled Polypropylene (PP) and Polyethylene (PE) for Intended Use in Different Plastics Processing Techniques, 2022.

Izenman, Alan Julian, 2013. Linear discriminant analysis. In: Izenman, Alan J. (Ed.), Modern Multivariate Statistical Techniques: Regression, Classification, and Manifold Learning. Springer New York, New York, NY, pp. 237–280. https://doi.org/10.1007/978-0-387-78189-1_8.

Jackson, J.E., 1991. A User's Guide to Principal Components. John Wiley & Sons, Inc., New York, London, Sydney.

Keshavarzi, N., Mashayekhy Rad, F., Mace, A., Ansari, F., Akhtar, F., Nilsson, U., Berglund, L., Bergström, L., 2015. Nanocellulose–zeolite composite films for odor elimination. ACS Appl. Mater. Interfaces 7, 14254–14262. https://doi.org/10.1021/acsami.5b02252.

Khanam, P.N., AlMaadeed, M.A.A., 2015. Processing and characterization of polyethylene-based composites. Adv. Manuf. Polym. Compos. Sci. 1, 63–79. https://doi.org/10.1179/2055035915Y.0000000002.

Kuchmenko, T., Umarkhanov, R., Lvova, L., 2020. E-nose for the monitoring of plastics catalytic degradation through the released Volatile Organic Compounds (VOCs) detection. Sensor. Actuator. B Chem. 322, 128585 https://doi.org/10.1016/j.snb.2020.128585.

Leslie, H.A., van Velzen, M.J.M., Brandsma, S.H., Vethaak, A.D., Garcia-Vallejo, J.J., Lamoree, M.H., 2022. Discovery and quantification of plastic particle pollution in human blood. Environ. Int. 163, 107199 https://doi.org/10.1016/j.envint.2022.107199.

Li, X., Wang, J., Guo, Y., Zhu, T., Xu, W., 2021. Adsorption and desorption characteristics of hydrophobic hierarchical zeolites for the removal of volatile organic compounds. Chem. Eng. J. 411, 128558 https://doi.org/10.1016/j.cej.2021.128558.

Lok, B., Buettner, A., Denk, P., Ortner, E., Fell, T., 2020. Exploring odor minimization in post-consumer plastic packaging waste through the use of probiotic bacteria. Sustain. Times 12, 1–18. https://doi.org/10.3390/su12229432.

Mark, J.E., 2007. Physical Properties of Polymers Handbook. Springer Science + Business Media, LLC. https://doi.org/10.1007/BF01840027.

Mutter, R., Stille, W., Strobl, G., 1993. Transition regions and surface melting in partially crystalline polyethylene: a Raman spectroscopic study. J. Polym. Sci., Part B: Polym. Phys. 31, 99–105. https://doi.org/10.1002/polb.1993.090310113.

Nel, H.A., Froneman, P.W., 2015. A quantitative analysis of microplastic pollution along the south-eastern coastline of South Africa. Mar. Pollut. Bull. 101, 274–279. https://doi.org/10.1016/j.marpolbul.2015.09.043.

Nerín, C., Aznar, M., Carrizo, D., 2016. Food contamination during food process. Trends Food Sci. Technol. 48, 63–68. https://doi.org/10.1016/j.tifs.2015.12.004.

Norris, J.F., 1932. The significance of pyrolysis temperatures. J. Chem. Educ. 9, 1890. https://doi.org/10.1021/ed009p1890.

Oleneva, E., Kuchmenko, T., Drozdova, E., Legin, A., Kirsanov, D., 2020. Identification of plastic toys contaminated with volatile organic compounds using QCM gas sensor array. Talanta 211, 120701. https://doi.org/10.1016/j.talanta.2019.120701.

Pabortsava, K., Lampitt, R.S., 2020. High concentrations of plastic hidden beneath the surface of the Atlantic Ocean. Nat. Commun. 11, 1–11. https://doi.org/10.1038/s41467-020-17932-9.

Patoski, A., 2019. Why Is most plastic not recycled? [WWW Document]. URL. https://repurpose.global/blog/post/why-is-most-plastic-not-recycled#:~:text=About 91%25 of plastic isn,not all can be recycled.

Pedregosa, F., Varoquaux, G., Gramfort, A., Michel, V., Thirion, B., 2011. Scikit-learn: machine learning in Python. J. Mach. Learn. Res. 12, 2825–2830. https://doi.org/10.1289/EHP4713.

Pelosi, P., 1996. Perireceptor events in olfaction. J. Neurobiol. 30, 3–19. https://doi.org/10.1002/(SICI)1097-4695(199605)30:1<3::AID-NEU2>3.0.CO;2-A.

Persaud, K., Dodd, G., 1982. Analysis of discrimination mechanisms in the mammalian olfactory system using a model nose. Nature 299, 352–355. https://doi.org/10.1038/299352a0.

[WWW Document] Polymer Market Analysis: Plant Capacity, Production, Operating Efficiency, Demand & Supply, Product Type, Application, Distribution Channel, Region, Competition, Trade, Market Analysis, 2015-2030, 2021. Polym. Mark. Size, Share | Glob. Ind. Anal. 2015-2030. URL. https://www.chemanalyst.com/industry-report/polymer-market-306.

Potyrailo, R.A., 2016. Multivariable sensors for ubiquitous monitoring of gases in the era of internet of things and industrial internet. Chem. Rev. 116, 11877–11923. https://doi.org/10.1021/acs.chemrev.6b00187.

Rahimi, A.R., Garciá, J.M., 2017. Chemical recycling of waste plastics for new materials production. Nat. Rev. Chem 1, 1–11. https://doi.org/10.1038/s41570-017-0046.

Rajendran, S., Scelsi, L., Hodzic, A., Soutis, C., Al-Maadeed, M.A., 2012. Environmental impact assessment of composites containing recycled plastics. Resour. Conserv. Recycl. 60, 131–139. https://doi.org/10.1016/j.resconrec.2011.11.006.

Raschka, S., 2015. Python Machine Learning. Packt Publishing Ltd., Birmingham.

Recycled plastics in food packaging [WWW Document] U.S. Food Drug Adm. URL. https://www.fda.gov/food/packaging-food-contact-substances-fcs/recycled-plastics-food-packaging.

Sanger, A., Kang, S.B., Jeong, M.H., Kim, C.U., Baik, J.M., Choi, K.J., 2019. All-transparent NO2 gas sensors based on freestanding Al-doped ZnO nanofibers. ACS Appl. Electron. Mater. 1, 1261–1268. https://doi.org/10.1021/acsaelm.9b00210.

Sangroniz, A., Zhu, J.-B., Tang, X., Etxeberria, A., Chen, E.Y.-X., Sardon, H., 2019. Packaging materials with desired mechanical and barrier properties and full chemical recyclability. Nat. Commun. 10, 3559. https://doi.org/10.1038/s41467-019-11525-x.

Schwartz-Narbonne, H., Xia, C., Shalin, A., Whitehead, H.D., Yang, D., Peaslee, G.F., Wang, Z., Wu, Y., Peng, H., Blum, A., Venier, M., Diamond, M.L., 2023. Per- and polyfluoroalkyl substances in Canadian fast food packaging. Environ. Sci. Technol. Lett. 10, 343–349. https://doi.org/10.1021/acs.estlett.2c00926.

Seitz, J.T., 1993. The estimation of mechanical properties of polymers from molecular structure. J. Appl. Polym. Sci. 49, 1331–1351. https://doi.org/10.1002/app.1993.070490802.

Sipos, L., Kovács, Z., Szöllősi, D., Kókai, Z., Dalmadi, I., Fekete, A., 2011. Comparison of novel sensory panel performance evaluation techniques with e-nose analysis integration. J. Chemom. 25, 275–286. https://doi.org/10.1002/cem.1391.

Tan, J., Xu, J., 2020. Applications of electronic nose (e-nose) and electronic tongue (e-tongue) in food quality-related properties determination: a review. Artif. Intell. Agric. 4, 104–115. https://doi.org/10.1016/j.aiia.2020.06.003.

Tharwat, A., 2016. Principal component analysis - a tutorial. Int. J. Appl. Pattern Recognit. 3, 197–240. https://doi.org/10.1504/IJAPR.2016.079733.

Tharwat, A., Gaber, T., Ibrahim, A., Hassanien, A.E., 2017. Linear discriminant analysis: a detailed tutorial. AI Commun 30, 169–190. https://doi.org/10.3233/AIC-170729.

Torri, L., Piergiovanni, L., Caldiroli, E., 2008. Odour investigation of granular polyolefins for flexible food packaging using a sensory panel and an electronic nose. Food Addit. Contam. 25, 490–502. https://doi.org/10.1080/02652030701513776.

Van Deventer, D., Mallikarjunan, P., 2002. Comparative performance analysis of three electronic nose systems using different sensor technologies in odor analysis of retained solvents on printed packaging. J. Food Sci. 67, 3170–3183. https://doi.org/10.1111/j.1365-2621.2002.tb08878.x.

Van Rensburg, M.L., Nkomo, S.L., Dube, T., 2020. The 'plastic waste era'; social perceptions towards single-use plastic consumption and impacts on the marine environment in Durban, South Africa. Appl. Geogr. 114, 102132 https://doi.org/10.1016/j.apgeog.2019.102132.

Van Toan, N., Tuoi, T.T.K., Inomata, N., Toda, M., Ono, T., 2021. Aluminum doped zinc oxide deposited by atomic layer deposition and its applications to micro/nano devices. Sci. Rep. 11, 1–12. https://doi.org/10.1038/s41598-020-80880-3.

Veerapandian, K.P., De Geyter N, S., Giraudon, J.-M., Lamonier, J.-F., Morent, R., 2019. The use of zeolites for VOCs abatement by combining non-thermal plasma, adsorption, and/or catalysis: a review. Catalysts. https://doi.org/10.3390/catal9010098.

Vera, L., Mestres, M., Boqué, R., Busto, O., Guasch, J., 2010. Use of synthetic wine for models transfer in wine analysis by HS-MS e-nose. Sensor. Actuator. B Chem. 143, 689–695. https://doi.org/10.1016/j.snb.2009.10.027.

Vera, P., Canellas, E., Nerín, C., 2020. Compounds responsible for off-odors in several samples composed by polypropylene, polyethylene, paper and cardboard used as food packaging materials. Food Chem. 309, 125792 https://doi.org/10.1016/j.foodchem.2019.125792.

Vollmer, I., Jenks, M.J.F., Roelands, M.C.P., White, R.J., van Harmelen, T., de Wild, P., van der Laan, G.P., Meirer, F., Keurentjes, J.T.F., Weckhuysen, B.M., 2020. Beyond mechanical recycling: giving new life to plastic waste. Angew. Chem. Int. Ed. 59, 15402–15423. https://doi.org/10.1002/anie.201915651.

Wiedmer, C., Velasco-Schön, C., Buettner, A., 2017. Characterization of off-odours and potentially harmful substances in a fancy dress accessory handbag for children. Sci. Rep. 7, 1–11. https://doi.org/10.1038/s41598-017-01720-5.

World, O., Day, E., Communications, N., 2018. The future of plastic. Nat. Commun. 9, 2157. https://doi.org/10.1038/s41467-018-04565-2.

Xu, M., Wang, J., Zhu, L., 2019. The qualitative and quantitative assessment of tea quality based on E-nose, E-tongue and E-eye combined with chemometrics. Food Chem. 289, 482–489. https://doi.org/10.1016/j.foodchem.2019.03.080.

Yates, J., Deeney, M., Rolker, H.B., White, H., Kalamatianou, S., Kadiyala, S., 2021. A systematic scoping review of environmental, food security and health impacts of food system plastics. Nat. Food 2, 80–87. https://doi.org/10.1038/s43016-021-00221-z.

Yu, H., Dai, X., Yao, G., Xiao, Z., 2014. Application of gas chromatography-based electronic nose for classification of Chinese rice wine by wine age. Food Anal. Methods 7, 1489–1497. https://doi.org/10.1007/s12161-013-9778-2.

Yüzay, I.E., Selke, S., 2007. Development of electronic nose method for evaluation of residual solvents in low-density polyethylene films. Packag. Technol. Sci. 20, 99–112. https://doi.org/10.1002/pts.745.

Zheng, J., Suh, S., 2019. Strategies to reduce the global carbon footprint of plastics. Nat. Clim. Change 9, 374–378. https://doi.org/10.1038/s41558-019-0459-z.